Photo-imageable Sol–Gel Hybrid Materials for Simple Fabrication of Micro-optical Elements

DONG JUN KANG AND BYEONG-SOO BAE*

Laboratory of Optical Materials and Coating (LOMC), Department of Materials Science and Engineering, Korea Advanced Institute of Science and Technology (KAIST), Daejeon 305-701, Republic of Korea

Received December 18, 2006

ABSTRACT

Special attention has been focused on photo-imageable sol–gel hybrid (SGH) materials because of their synergetic effects, such as high photosensitivity and transparency, as well as mechanical and chemical durability resulting from the presence of polymer and silica networks in the hybrid structure. Photo-induced migration, which accompanies photopolymerization and photolocking in these materials, allows for the formation of convex micropatterns with a higher refractive index than the original film through exposure to UV radiation. Controlling the parameters affecting this photo-induced migration can permit modulation of the size and shape of such microstructures for the simple and cost-effective direct photofabrication of micro-optical elements, such as microlenses and microlens arrays.

1. Introduction

The phenomenon of photosensitivity and, in particular, the possibility of inducing a permanent change in the refractive index and/or volume of a medium by exposing it to light have attracted attention because of their potential application in the direct photofabrication of micro-optical elements, such as microlenses, microlens arrays, optical waveguides, and diffractive optical elements.[1–22] To date, micro-optical elements have most commonly been fabricated using multistep methods, such as lithographic or etching techniques.[23] These methods, however, are often complex and require several steps to be undertaken before the desired surface structure is revealed, thus placing limitations on the prospect of the straightforward, low-cost production of micro-optical elements. The introduction of photosensitive materials, which could be patterned by simply exposing them to light, offers the prospect of a considerable improvement over conventional methods. As a result, the characteristics of many photosensitive materials, such as inorganic glasses,[7–10] photopolymers,[1–4] and azopolymers,[6] have been investigated. The photosensitive inorganic glasses, however, exhibit very small changes in the refractive index and volume, thereby limiting their application in the manufacture of optical elements. On the other hand, photo- and azopolymers would need to be modified in such a way that they demonstrate higher thermal stability and optical transparency than they currently possess if they are to be used in the production of micro-optical elements.

An alternative can be found in recent reports on the use of newly developed photo-imageable sol–gel hybrid (SGH) materials for practical applications.[11–22] These materials have been demonstrated to exhibit high sensitivity to UV radiation, a property which can be directly exploited to permit the fabrication of micro-optical elements. In comparison to other photosensitive materials, SGH materials exhibit higher photosensitivity levels and, perhaps even more importantly, these levels are controllable to a significant degree. This control is achieved through the deliberate variation of parameters, such as the composition of the material, the UV wavelength used during the exposure process, and other process parameters. In addition, synergetic effects as a result of interactions between the inorganic and organic components in the materials have been shown to enhance various characteristics of SGH materials.[12] The photo-excitation of the azobenzene group in SGH materials by polarized light can create surface relief gratings on the films with a high birefringence.[11] However, in the photo-imageable SGH materials, various mechanisms based on the presence of an inorganic siloxane group and a polymerizable organic group or doped photo-active organic monomers have been proposed to explain different types of photo-induced self-structuring on the material surface. The most common suggestions are that either a combination of organic polymerization[14,15] and inorganic condensation or a process of densification[13] is responsible. Either of these could cause the observed behavior of volume shrinkage accompanied by an increase in the refractive index. However, the different behavior of volume expansion with a refractive index increase has also been observed in combination with various surface modulations when photo-imageable SGH materials are exposed to UV radiation. In the first instance, the combination of volume expansion and a large increase in the refractive index was found in SGH materials that had been doped with a large quantity of photo-initiator.[16] This was explained through a proposed "photolocking" mechanism, which involved the attachment of photodecomposed radicals from the photo-initiator to the host SGH matrix. This mechanism can explain the observed refractive index increase, which is a linear function of the photo-initiator

Dong Jun Kang received his B.S. degree in 2001 from Pusan National University in Korea, followed by a M.S. degree in 2003 and a Ph.D. degree in 2006, both of which were from Korea Advanced Institute of Science and Technology (KAIST) under the supervision of Professor Byeong-Soo Bae. He is currently a postdoctoral fellow at the National Institute of Advanced Industrial Science and Technology (AIST) in Japan. His research interests include sol–gel-derived organic–inorganic hybrid materials for the fabrication of micro- and nanostructures.

Byeong-Soo Bae received his B.S. degree in 1986 from Seoul National University in Korea, his M.S. degree in 1988 from Drexel University, and his Ph.D. degree in 1993 from the University of Arizona under the supervision of Professor Michael C. Weinberg. He has been a faculty member of the Department of Materials Science and Engineering in Korea Advanced Institute of Science and Technology (KAIST) since 1994. Currently, he is a director of the Sol–Gel Innovation Project (SOLIP) funded by the Korean government and industries. His research interests include sol–gel-derived organic–inorganic hybrid materials and fabrication processes for application to optics and displays.

* To whom correspondence should be addressed. Fax: 82-42-869-3310. E-mail: bsbae@kaist.ac.kr.

10.1021/ar6000439 CCC: $37.00
Published on Web 06/14/2007

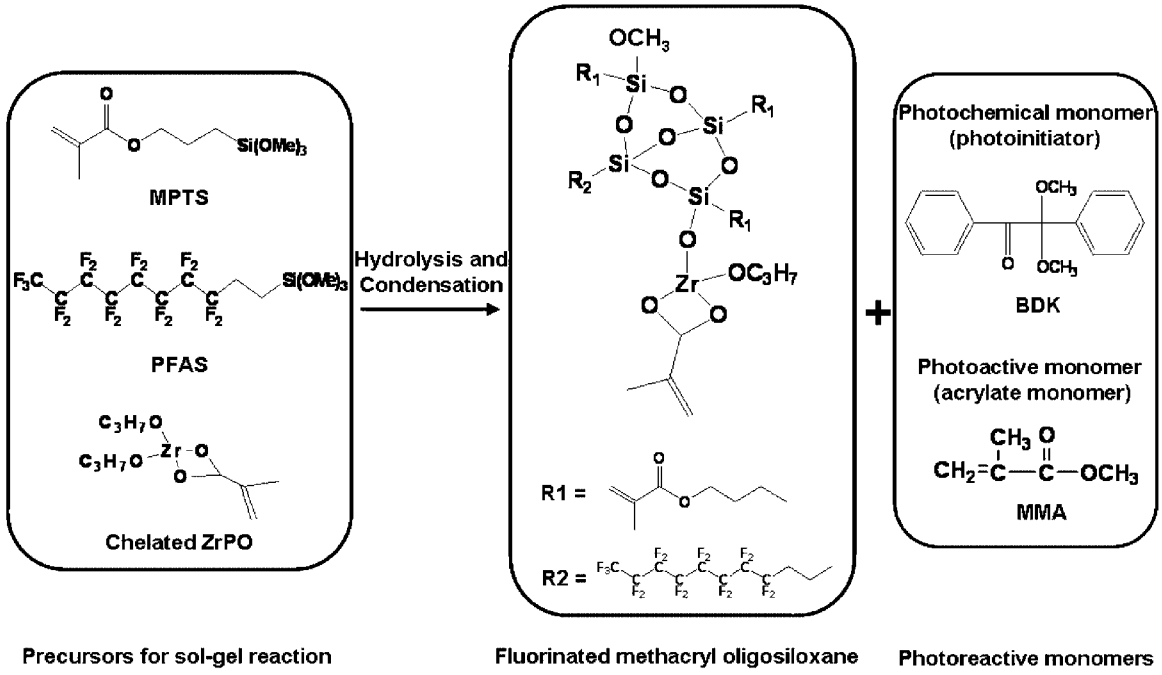

FIGURE 1. Schematic diagram of major components and synthesis of photo-imageable SGH material.

concentration, but it does not sufficiently explain the observed high level of volume expansion that occurs when the material is selectively illuminated. As a result, some researchers have proposed the migration of constituents from exposed areas to unexposed areas in SGH materials because of the presence of a chemical composition gradient induced by photo-induced reactions that, of course, occur only in the exposed area.[18–22] This behavior had already been observed in photopolymers,[1–5] which mainly consist of a polymerized binder matrix, a photo-active monomer, and a solvent. In this case, however, the extent of the migration was low because the gradient in the chemical composition between the exposed area and the unexposed area was small because of the presence of the polymerized binder matrix within the photopolymer. Moreover, the practical application of photo- and azopolymers in the creation of micro-optical elements was restricted because of their low thermal durability and poor optical transparency.

Photo-imageable SGH materials should not experience the problems associated with photopolymers, and they exhibit extensive photo-induced migration as a result of the various photo-induced reactions mentioned above. However, thus far, the existence of a photo-induced migration mechanism has not been confirmed either in photosensitive SGH materials or in photopolymers. This Account describes the first observation of in situ microstructural evolution as a function of UV exposure dosage, thus demonstrating identifiable migration behavior in a photo-imageable SGH material. Also, the impact of changes in the parameters affecting this photo-induced migration on the microstructural evolution of the material is discussed, particularly with reference to the possibility of manipulating these parameters to control the shape of microstructures that could be used in the photofabrication of micro-optical elements, such as microlenses and microlens arrays.

2. Design and Synthesis of Photo-imageable SGH Material

Because it is reasonable to expect many photo-induced reactions in materials containing methacrylate, it has been common to synthesize methacrylate SGH materials using 3-trimethoxysilylpropyl methacrylate (MPTS). Our photo-imageable SGH material was newly designed and synthesized with an eye toward inducing high levels of photo-induced migration of monomers and oligomers in subsequent fabrication processes.[18,22] A large quantity of a photochemical monomer (i.e., a photo-initiator or other photodecomposable monomer) and a photo-active monomer (i.e., a polymerizable acrylate monomer) was added to enhance photo-induced reactions in the SGH material. Figure 1 illustrates schematically the major components of this photo-imageable SGH material. MPTS, heptadecafluorodecyltrimethoxysilane (PFAS), zirconium *n*-propoxide (ZPO), and methacrylic acid (MAA) were used as starting materials for the formation of fluorinated methacryl-oligosiloxane in the solution. On the basis of the sol–gel reaction, hydrolysis of alkoxysilanes in the existence of water followed by condensation of hydroxyl groups forms the siloxane.[24] The reaction is sensitive to the alkoxysilane composition, amount of water, catalysis, and temperature. Here, PFAS was used to improve the optical transparency of the material through fluorination of the methacryl-oligosiloxanes, and ZPO was used to catalyze the sol–gel reaction and thus to encourage the formation of highly condensed oligosiloxanes. Also, when the amount of PFAS and ZPO used in the reaction is controlled, it is possible to tune the refractive index of the

fabricated SGH material as required. For our study, the MPTS and PFAS were first hydrolyzed with 0.75 equiv of 0.01 M hydrochloric acid (HCl). ZPO was then reacted with MAA in a molar ratio of 1:1 to form a chelating complex in a N_2 atmosphere. After that, the chelated ZPO solution was added to the prehydrolyzed MPTS and PFAS solution and stirred for 1 h to advance hydrolysis and condensation. The mixed solution was reacted with additional water for 20 h to complete the hydrolysis and condensation reactions. The total amount of water contained 1.5 equiv of total alkoxides in the solution. After the reaction to synthesize the fluorinated methacryl-oligosiloxane solution, any residual products (such as alcohols) were removed at 50 °C with an evaporator. Solid benzyldimethylketal (BDK) (a photochemical monomer) dissolved in methylmethacylic acid (MMA) (a photo-active monomer) was added to the fluorinated methacryl-oligosiloxane solution. Here, the photochemical monomer, BDK, has roles in both the initiation of the photopolymerization and doping of the photolocking agent after its photodecomposition. The photo-active monomer, MMA, acts as either a polymerizable group in areas of the material exposed to UV radiation or as a diffusible group in unexposed areas. It also acts as a solvent for the large BDK content. The resulting photo-imageable SGH material is optically transparent because of the highly condensed fluorinated methacryl-oligosiloxane base structure and is highly photosensitive because it contains high levels of both the photo-initiator and the acrylate monomer. The polymerized SGH material is dense, without the presence of micropores, enough to be used in optics because of the additional cross-linking of oligosiloxanes. The glass transition has not been found below the decomposition temperature, which is over 300 °C, and the negligible birefringence ($<10^{-2}$) can be reserved during heating and cooling.[25] These robust characteristics can allow SGH material to be used in many optical applications.

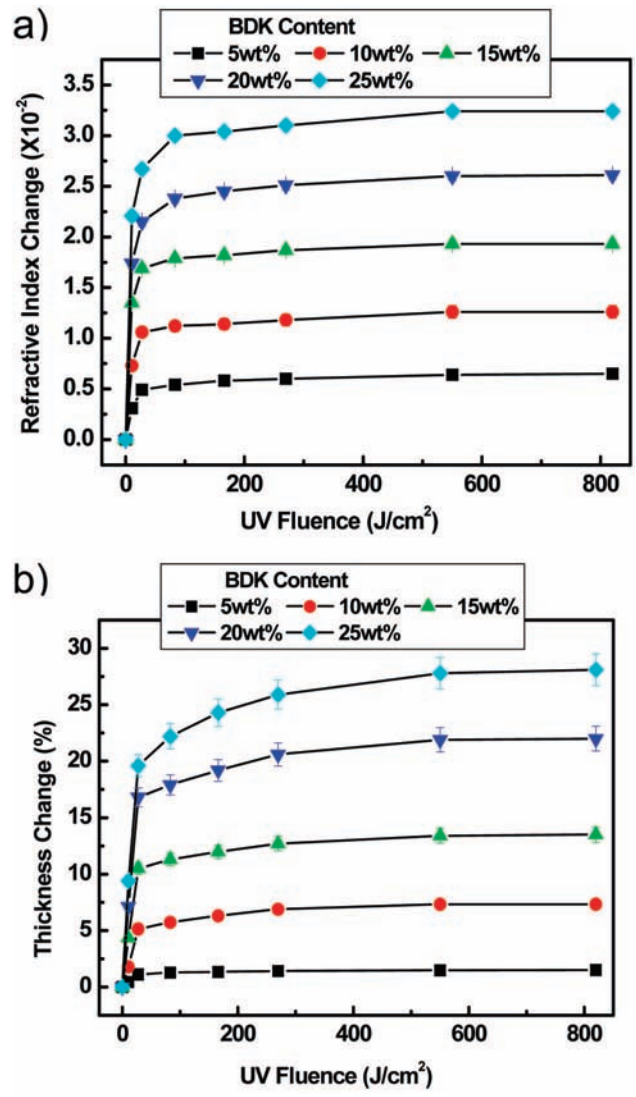

FIGURE 2. Changes in the refractive index (a) and thickness (b) of UV-exposed SGH films as a function of the UV dose and BDK content. The films were baked at 150 °C for 3 h after UV exposure.

3. Photosensitivity of Photo-imageable SGH Materials

Figure 2 shows the changes in the refractive index (a) and thickness (b) of various SGH films as a function of the UV exposure dose and BDK content. Regardless of the BDK content, both the refractive index and the film thickness increase rapidly for short UV exposures and then become saturated. Their saturated values provide a measure of the photosensitivity of the material. Photopolymerization as well as photolocking accompanied by photodecomposition of the BDK is fast for UV illumination with high power ratings. Generally, photopolymerization induces volume shrinkage along with a small increase of the refractive index. As we have demonstrated in previous reports,[16] the main cause of the observed increases in both the refractive index and film thickness in SGH materials is a photolocking mechanism that fixes the photodecomposed radicals from the BDK into the methacryl-oligosiloxane matrix. This was established by comparing the refractive index and thickness of films, whose photodecomposition products (highly polar radicals) are fixed in exposed areas to the thickness and refractive index of unexposed film in which BDK is volatilized during thermal baking. It has become clear that increases in the refractive index and film thickness are each enhanced in a way that is proportional to the BDK content (see Figure 2). In other words, considerably higher photosensitivity can be obtained in these materials if their composition is modified to contain high levels of BDK. In the past, the restricted solubility of BDK in the organo-oligosiloxane solution has been a limiting factor in the ability to dope sol–gel films of this sort with large amounts of BDK. In this study, however, large quantities of BDK were dissolved in MMA, which is a photo-active monomer, to participate in the photopolymerization of the methacrylate and to act as a source of mobile (and hence able to diffuse and migrate) monomers. We have found that a composition that made use of 25 wt % BDK dissolved in 15 wt % MMA exhibits the highest photosensitivity. That is, such films demon-

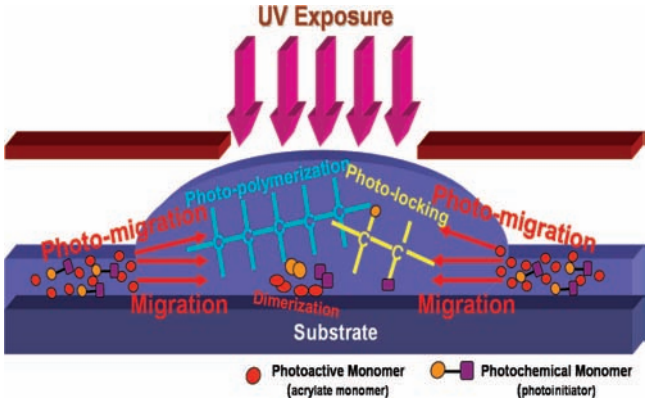

FIGURE 3. Schematic diagram of the photo-induced migration mechanism in SGH materials during selective UV exposure with a photomask.

strate the largest changes in both the refractive index (over 10^{-2}) and film thickness (about 30%) upon UV exposure (see Figure 2).

4. Photo-imaging of SGH Materials

4.1. Photo-induced Migration Mechanism. Figure 3 is a schematic diagram of the photoinduced migration mechanism in photo-imageable SGH materials. Whether the selective UV illumination is accomplished using a photomask or direct laser writing, the exposed area experiences various photo-induced reactions. First of all, BDK is readily decomposed to two radicals that initiate the photopolymerization of the methacryl-oligosiloxanes and MMA. This photopolymerization includes processes such as oligopolymerization, low-order polymerization, homopolymerization, and copolymerization. Also, the photodecomposed radicals are fixed in the methacryl-oligosiloxane matrix or undergo a dimerization process in which two benzoyl radicals form benzil molecules, as described in a previous study.[26] The cross-linking and attachment of doped molecules in the UV-exposed area of the SGH film differentiate these areas from the mixed state of oligomers and monomers in the unexposed areas. This structural distinction causes substantial differences between the concentration of unreacted molecules in exposed and unexposed areas, as well as in the diffusivity and the molecular size and weight of the constituents in these areas. The result is a chemical composition gradient between the exposed and unexposed areas, making it thermodynamically preferable for unreacted oligomers or monomers to migrate into the exposed area, where they then react via photopolymerization or photolocking. This migration will continue until all available sites for polymerization and photolocking in the exposed area are consumed or until the diffusivity of the oligomers or monomers in the unexposed area drops below the level necessary to drive it. Thermal baking of the SGH film after the UV exposure stabilizes the film, allowing it to be imaged clearly. The heating may polymerize the methacryl oligomers and MMA monomers in the film and may also remove any nondecomposed BDK in the unexposed area by evaporation.[17] This latter process is likely to occur because of the intrinsic high diffusivity and volatility of BDK. In any case, thermal baking hardens the surface of the exposed regions, preventing further migration of either oligomers or monomers. In this way, stabilized surface structures with expanded volumes and higher refractive indices are formed in the exposed region.

To further elucidate the processes proposed in this schematic, changes in the molecular structure of the films in micropatterned areas were mapped using a Fourier transform infrared spectroscopy (FTIR) microscope in combination with an IR spectroscope and an optical microscope. Figure 4a shows an optical micrograph of a circular microstructure of approximately 80 μm in diameter detected using white-light illumination and the FTIR microscope. A FTIR step scan was conducted across the circle with a scanning length of approximately 110 μm and 8 spectral steps. The results are shown in Figure 4b. Because the photo-imageable SGH films had not been dried prior to the scan, it was assumed that any observed changes in the molecular structure were only due to photoreactions. It appears that the intensity of the $\nu_{C=C}$ peak at 1638 cm^{-1} reduces, and the $\nu_{C=O}$ peak at 1719 cm^{-1} shifts to longer wavenumbers as the IR-scanning position moves from the edge of the circle to its center. This represents the consumption of C=C bonds and the loss of conjugation with the C=C bond because of photopolymerization or photolocking and is proportional to the variation in the intensity distribution of the original UV exposure. On the other hand, the integrated area of the $\nu_{C=O}$ band at 1719 cm^{-1} remains constant. The conversion degree of the C=C bond calculated from the integrated peak intensities of the $\nu_{C=C}$ and $\nu_{C=O}$ bands[27] was plotted against the scanning position, as well as the $\nu_{C=C}$ peak intensity (see Figure 4c). The conversion degree of the C=C bond increases up to 96% in the center of the exposed region, indicating intensive photo-induced reactions and affirming the modulation of the molecular structure that will result in a substantial chemical composition gradient. Because this modulation follows the intensity profile of the UV beam used for the original exposure, it follows that the gradient should follow this profile as well and, subsequently, induces the migration of unreacted monomers or oligomers from unexposed areas (low-conversion degree) to exposed areas (high-conversion degree).

The modulation in the grade of the photo-induced reactions depending upon the UV exposure intensity may produce the refractive index profile across the photofabricated pattern. The refractive index modulation of the pattern was measured using a near-field scanning optical microscope (NSOM) in reflection mode with an Ar laser ($\lambda = 488$ nm) as the probing source. Figure 5 shows some 2D NSOM line profiles of the optical intensity of the reflection (which represents the refractive index modulation of a photofabricated object) on the SGH films. Three differently shaped regions were exposed. Figure 5a shows a microstructure in the shape of a simple line. Figure 5b is a single circle, while Figure 5c is an image of an array of circles. It is clear that the refractive index modulation

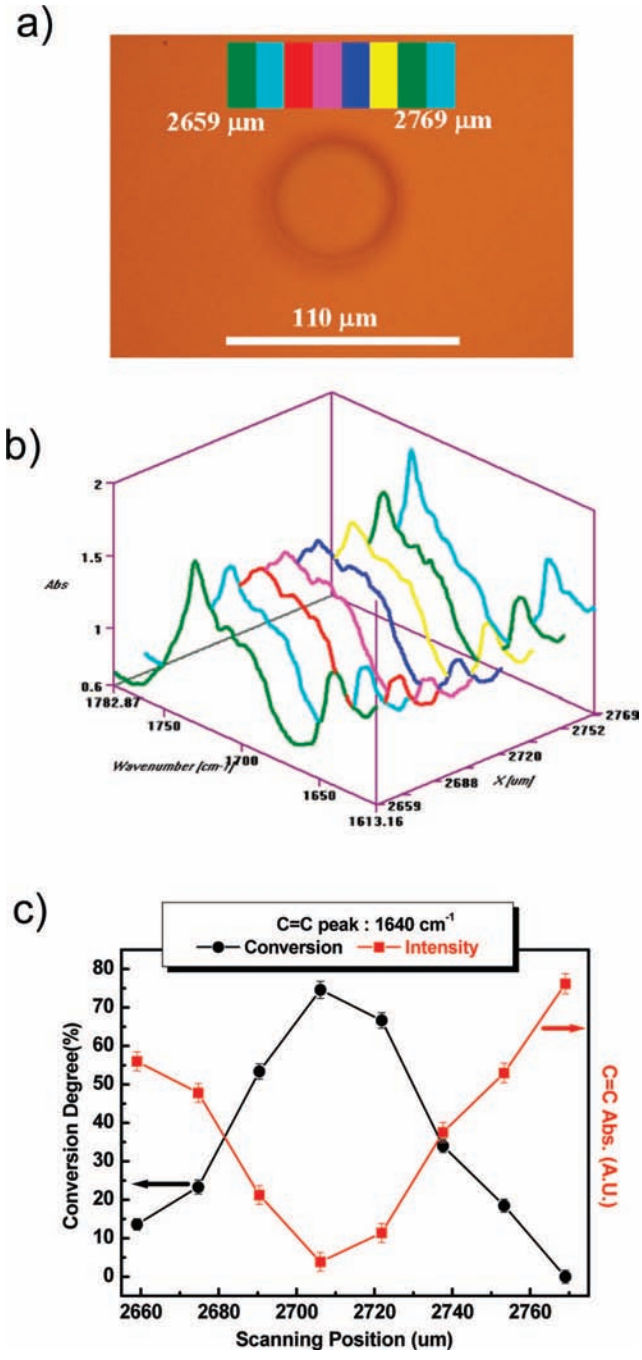

FIGURE 4. (a) Optical micrograph of a circular microstructure on a SGH film detected using white light and a FTIR microscope. The circle of approximately 80 μm in diameter was fabricated using a binary photomask with a diameter of 30 μm. (b) FTIR mapping spectra of 8 steps across the circle with a scanning length of approximately 110 μm. (c) Profiles obtained from the FTIR spectra of the conversion degree and C=C peak intensity as a function of the IR-scanning position across the circle.

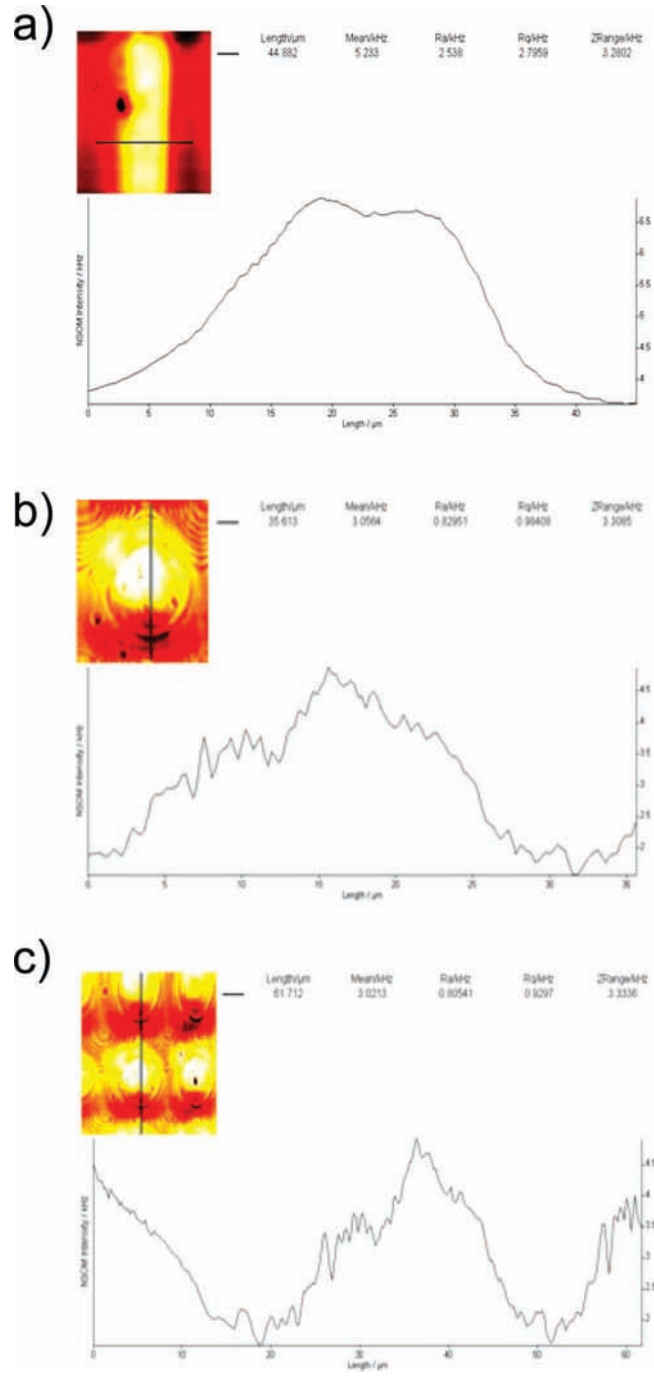

FIGURE 5. Two-dimensional NSOM line profiles of the optical intensity representing the refractive index profiles of photofabricated microstructures on SGH films that were (a) line-shaped, (b) circular, and (c) an array of circles.

follows the topological shape of the photofabricated patterns in all of the microstructures. This modulation occurs because of the photo-induced reaction profile that was inferred from the molecular structure changes evident in the FTIR scans.

To confirm the proposed photo-induced migration empirically, we analyzed the microstructural evolution of the surface of the micropatterns on the SGH films during selective UV exposure in situ. Figure 6 shows a set of 3D scanning interferometer (SI) images of (a) circle- and (b) line-shaped surface microstructures as a function of the UV dose. The diameter of the circle and the line width of the binary photomasks used during the exposure were 30 and 10 μm, respectively. The photofabricated circle- and line-shaped surface structures exhibit various modulations as the UV dose increases. As can be seen, both structures have only a single peak as a result of the initial UV dose. The irradiated area becomes fixed and hardened because of the occurrence of intensive photo-induced reactions.

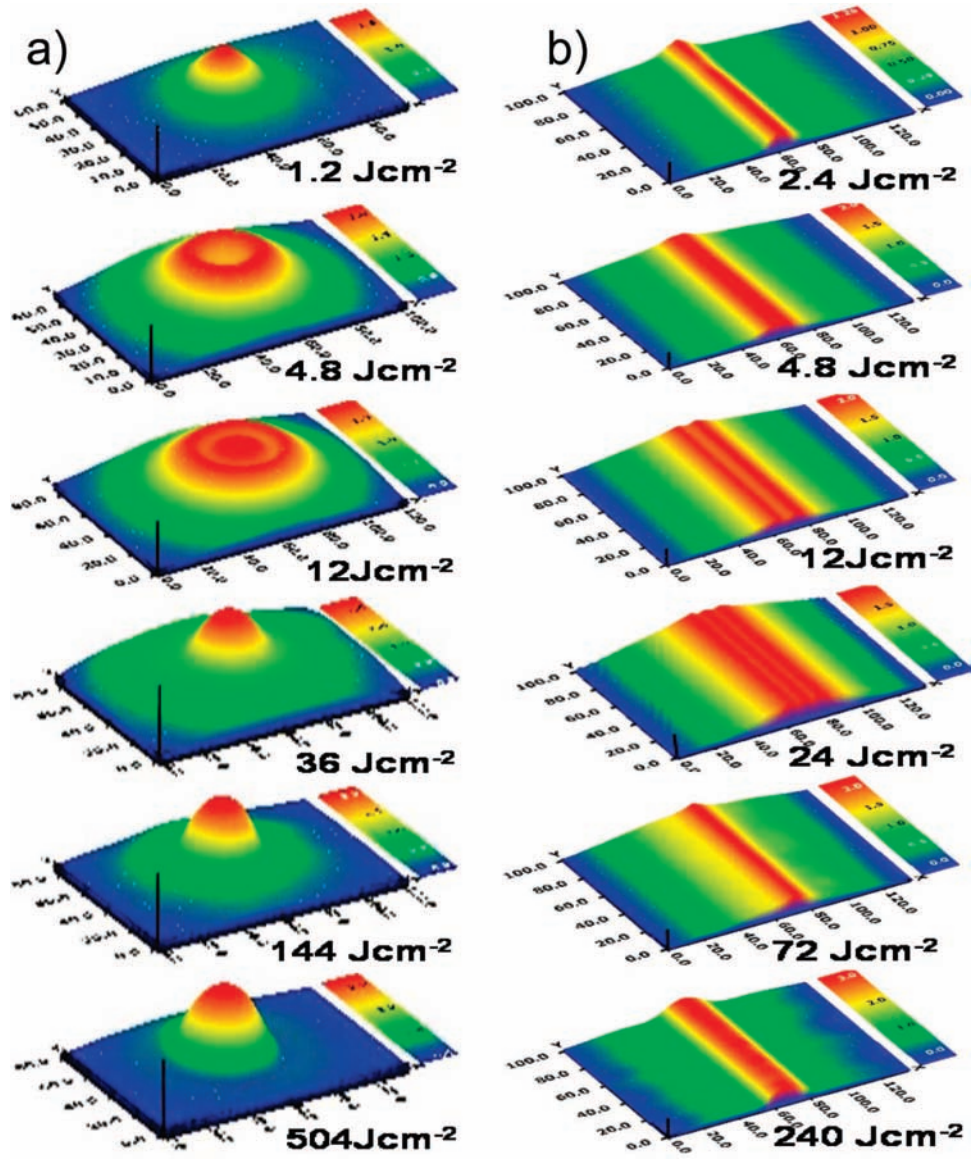

FIGURE 6. Three-dimensional SI images of in situ surface microstructural evolution of (a) circle-shaped (30 μm in diameter) and (b) line-shaped (10 μm in width) micropatterns on photo-imageable SGH films as a function of the UV exposure dose.

As the UV dose grows, the micropatterns in the exposed areas evolve into more complex shapes because of the relative depression of the central areas. This depression is the result of the migration of oligosiloxanes and unreacted monomers from the unexposed sides, which increases the height of the film around the exposed region. The migration continues, shifting the peaks toward the center and causing the uplift of the hardened central area along with the formation of another shoulder around the exposed area. This constant migration thus shapes the micropatterns into three peaks. Finally, even more migration combines the three peaks to form the single shape (either a line or a circle). After this point, the width and height of the photofabricated pattern are enhanced because of more migration, but the shape of the structure no longer changes. This in situ surface microstructural evolution in the photofabricated micropatterns (single pattern → double patterns → triple patterns → unified single patterns → pattern growth) convincingly demonstrates the migration behavior of the constituents from the unexposed area to the exposed area. It is to be expected that the migration is dependent upon various composition and process parameters, which would result in variation in the microstructural evolution of a given film as a function of the UV exposure dose. By understanding this behavior, we can control the shape of the photofabricated microstructures to produce a range of micro-optical elements.

4.2. Photo-induced Migration Parameters and Controllability. On the basis of the SI images in Figure 6, we numerically analyzed the surface modulation of the photofabricated circle- and line-shaped microstructures as a function of the UV dose. Figure 7 presents the height and width changes of the (a) circle- and (b) line-shaped structures as the UV dose was increased. The heights of the circle and line patterns increase steeply in the initial UV dose ranges and then grow slowly at higher dosage levels. On the other hand, the width of both the circle and

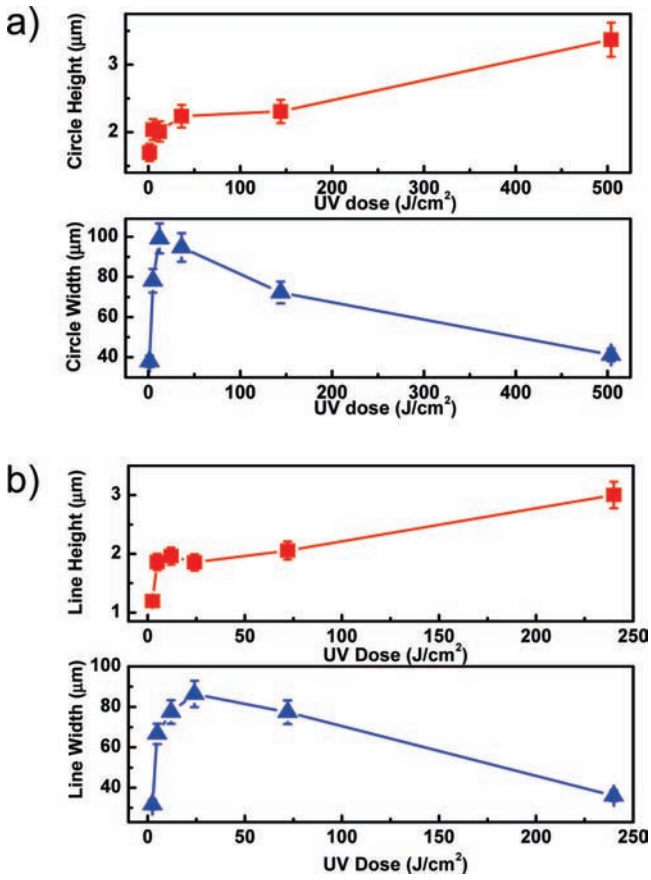

FIGURE 7. Changes in the height (■) and width (▲) of photofabricated surface microstructures of (a) circle- and (b) line-shaped micropatterns on SGH films.

the line patterns decrease drastically after climbing steeply during the initial exposure. This suggests that the photo-induced reactions in the exposed area are strongly active during short UV doses. The high levels of activity result in sudden surface modulations, with increasing pattern widths and heights because of rapid migration of material from the unexposed area to the exposed area. After this initial period of rapid migration, further migration occurs more slowly, raising the height of the structure but concentrating the movable species into the central region, thus narrowing the width of the pattern. Careful control of the UV dose, then, permits the design of micro-optical elements of well-defined height and width.

In addition to the UV exposure dose, the impact of other parameters on the photo-induced migration process in SGH materials can be considered. These include the concentration of photosensitive monomers in the film, the original film thickness, and area of the exposed site. Figure 8 summarizes the surface evolution of the photo-fabricated patterns as functions of these parameters. It is apparent that this evolution is both complicated and very sensitive to changes in any of the parameters tested. As we have already discussed, higher levels of BDK in the SGH material induce a steeper chemical composition gradient and lead to more active photo-induced migration. As a result, increasing the concentration of BDK leads to greater maximum heights in the final microstructure. Similarly, the presence of higher numbers of oligomers

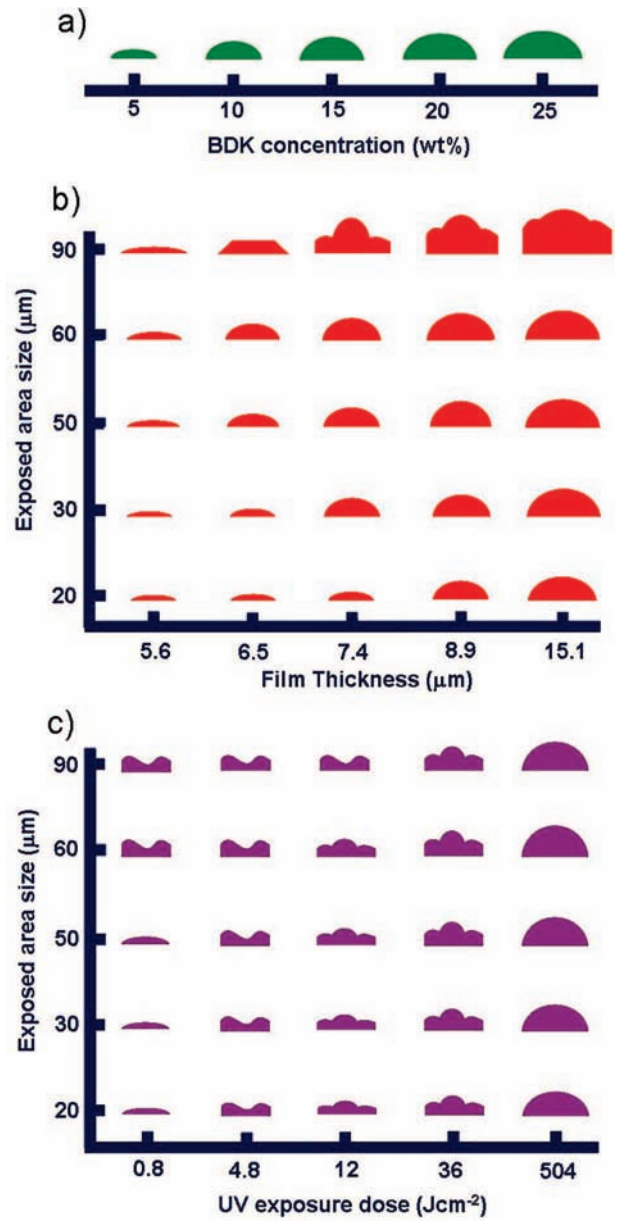

FIGURE 8. Mapping of the structural evolution of the surface of microelements as a function of photo-induced migration parameters: (a) concentration of BDK, (b) film thickness versus exposed area size, and (c) UV exposure dose versus exposed area size.

or monomers (i.e., more molecules available for diffusion and migration) in the thicker films leads to increased maximum heights. Thus, for a given pattern width, higher surface structures are obtained by using thicker films of photo-imageable SGH materials containing more oligosiloxane and photosensitive monomers (i.e., more BDK and MMA).

Because the migration required for the creation of these microstructures is a kinetic phenomenon, the migration length is limited to the fabrication of convex microstructures and the achievable microstructure size may be restricted. The resulting profile of any photofabricated microstructure is highly dependent upon the size of the exposed area, as evident in parts b and c of Figure 8. For large exposed areas, more photoinduced migration is required to achieve the desired convex shape typical of a

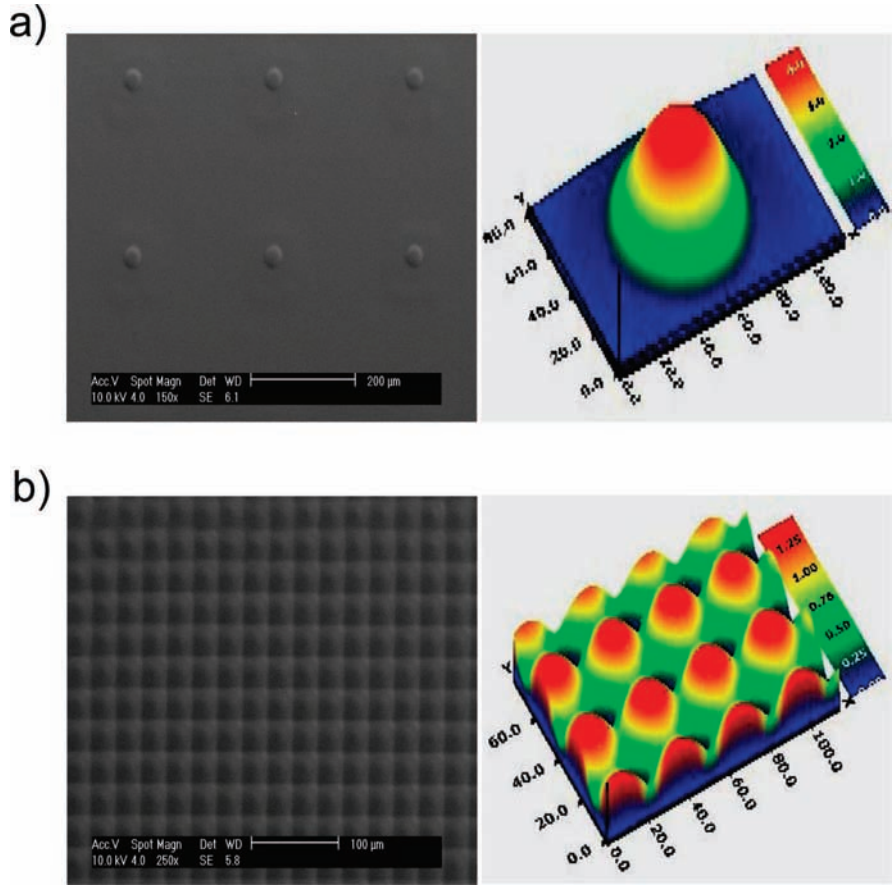

FIGURE 9. SEM and 3D SI images of a (a) microlens (40 μm in diameter and 3.2 μm in height) and (b) microlens array (30 μm in diameter and 1.25 μm in height) directly photofabricated on SGH films.

lens, for example. As a result, the creation of structures with larger areas will require the use of films with either higher concentrations of photosensitive monomers or greater film thickness or will involve the use of longer exposure times to permit sufficient migration levels to generate the desired shape. In addition, the dimension of the unexposed area should be large compared to the exposed area, thus providing an abundant source of migrating monomers.

The careful consideration of the effect of variation in both composition and process parameters upon the photofabricated microstructures has permitted a clearer understanding of the photo-induced migration process. Moreover, it is apparent that the well-shaped microstructures that are desirable in various micro-optical elements can be readily formed by precisely controlling these parameters. Thus, photo-imageable SGH materials permit very efficient and flexible patterning with excellent potential for applications in the direct photofabrication of micro-optical elements.

5. Direct Photofabrication of Microlenses and Microlens Arrays

It has been reported that many micro-optical elements, such as diffraction gratings and optical waveguides, have been directly photofabricated using photo-imageable SGH films.[13–21] Microlenses and microlens arrays can also be directly photofabricated on these films by the precise control of the parameters affecting photo-induced migration within the films.[22] SGH films were selectively illuminated under a Hg UV lamp using a binary photomask containing microlenses and microlens-array patterns of various sizes. In a single fabrication step, the UV exposure formed the desired convex microlenses and microlens arrays without the need for any etching or developing processes. Figure 9 represents the scanning electron microscopy (SEM) (left) and 3D SI (right) images of photofabricated (a) microlenses and (b) microlens arrays on SGH films. Through the precise control of the photo-induced migration mechanism, convex microlenses and microlens arrays with diameters of 40 and 30 μm and heights of 3.2 and 1.25 μm, respectively, were designed and directly photofabricated. The fabricated optical elements exhibit good homogeneity in addition to the required refractive index distribution. Also, the surface roughness of the fabricated elements was as low as around 0.5 nm root mean square (rms). This is within the value required for the elements to be optically applicable and is equivalent to that of the unexposed area. This is a result of the fact that no etching or developing process was required and the excellent coating qualities of the SGH, despite its high concentration of BDK. The good surface quality of the fabricated microlens and microlens array opens the way for many potential applications in fields such as optical communications and efficiency enhancing display layers.

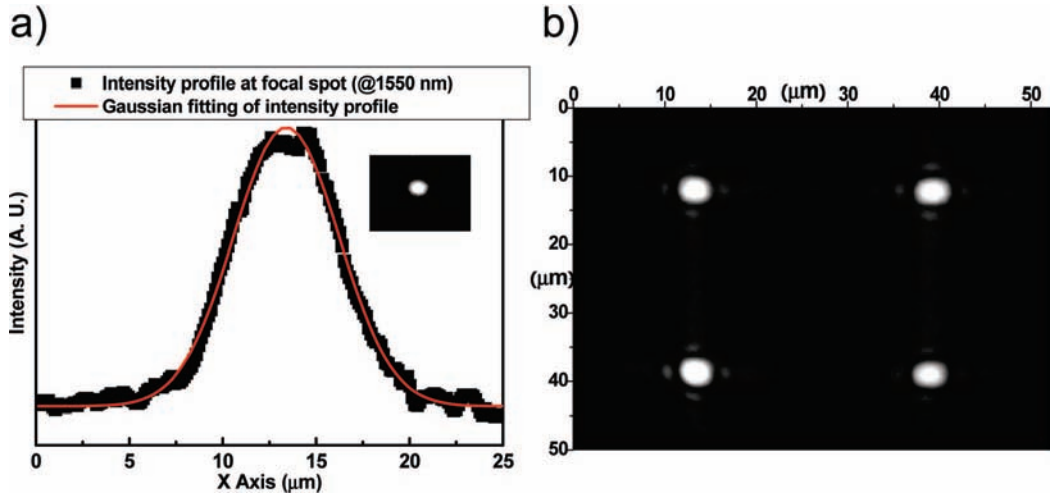

FIGURE 10. Focusing properties in the focal plane of a microlens and microlens array directly photofabricated on SGH films. (a) Focusing profiles at the focal spot of the microlens (focal spot image is shown in the inset) and (b) focal spot image at the focusing plane of the microlens array.

We evaluated the focusing properties of the micro-optical elements in the focal plane with a beam profiler, using a 1550 nm laser source and a charge-coupled device (CCD). A microlens with a diameter and height of 105 and 2.25 μm, respectively, was used. The spot diameter based on the $1/e^2$ intensity of the peak and found by fitting a Gaussian to the profile was 11.3 μm. The focal length was measured to be 350 μm. A microlens array was also characterized. The diameter and height of each component lens was 60 and 3.46 μm, respectively. In this case, the spot diameter was 3.98 μm and the focal length was measured to be 155 μm. As is illustrated in Figure 10, the distinctive beam profile of a microlens, demonstrating a good fit to a Gaussian profile, was found. Also, the image of the beam focused through a 2×2 array of microlenses exhibits excellent uniformity in the profiles because of the high refractive index distribution and controlled surface modification discussed earlier. Moreover, because the refractive index distribution as well as both the size and shape of the microlens are readily controlled, the focal lengths of the microlenses produced can be tuned. Similarly, focusing properties such as the fill factor and focusing beam homogeneity can be enhanced through more precise control of the photo-induced migration parameters, which should be particularly useful in the simple production of various micro-optical elements.

6. Conclusions and Prospects

SGH materials exhibit high levels of photosensitivity that are related to strong photo-induced reactions, such as photopolymerization and photolocking. These reactions cause photo-induced migration that results in efficient modification of the refractive index and volume of the material, permitting the simple fabrication of micro-optical structures. The formation of the microstructures on the film surfaces was found to be highly dependent upon many composition and process parameters, such as the UV dose, concentration of photosensitive molecules in the film, film thickness, and exposed area size. Through in situ observations of the evolution of various photofabricated patterns as a function of the UV dose and other parameters, we have been able to confirm the occurrence of photo-induced migration of molecules from unexposed to exposed areas on the films. Finally, well-defined and high-performance microlenses and microlens arrays with smooth surfaces were designed and directly fabricated through the precise control of this photo-induced migration process. The direct photofabrication of micro-optical elements using the photo-imageable SGH material described has potential applications in the simple production of various micro-optical elements used in optics and displays.

Micro-optical technology has thus far been used in high-performance applications rather than in mass production because of its high cost. Recently, many industrial applications have demonstrated a need for micro-optical technologies at low cost. Thus, the development of cheap materials and simple fabrication technologies for the production of micro-optical elements is required. It has been found that SGH materials possess many advantageous characteristics for optical applications compared to other optical materials, such as glasses and polymers. In addition to the superior optical characteristics of these materials, the simple and direct photofabrication of micro-optical elements using them provides the potential for cost-effective technology that can be readily applied in mass-production industries. For the practical application of the photo-imageable SGH materials, it is necessary to identify suitable industrial applications and demonstrate the simpler fabrication of many micro-optical elements with good reliability and characteristics acceptable in the current market.

This work was supported by the Korea Science and Engineering Foundation (KOSEF) Grant funded by the Korean government (MOST) (R01-2003-000-10125-0).

References

(1) (a) Colburn, W. S.; Haines, K. A. Volume hologram formation in photopolymer materials. *Appl. Opt.* **1971**, *10*, 1636–1641. (b) Trout, T. J.; Schmieg, J. J.; Gambogi, W. J.; Weber, A. M. Optical photopolymers: Design and applications. *Adv. Mater.* **1998**, *10*, 1219–1224.

(2) (a) Booth, B. L. Photopolymer material for holography. *Appl. Opt.* **1975**, *14*, 593–601. (b) Booth, B. L.; Marchegiano, J. E.; Chang, C. T.; Furmanak, R. J.; Graham, D. M.; Wagner, R. G. Polyguide polymeric technology for optical interconnect circuits and components. *Proc. SPIE—Int. Soc. Opt. Eng.* **1997**, *3005*, 238–251.

(3) (a) Tomlinson, W. J.; Kaminow, I. P.; Chandross, E. A.; Fork, R. L.; Silfvast, W. T. Photoinduced refractive index increase in poly(methylmethacrylate) and its applications. *Appl. Phys. Lett.* **1970**, *16*, 486–489. (b) Chandross, E. A.; Pryde, C. A.; Tomlinson, W. J.; Weber, H. P. Photolocking—A new technique for fabricating optical waveguide circuits. *Appl. Phys. Lett.* **1974**, *24*, 72–74.

(4) (a) Franke, H. Optical recording of refractive-index patterns in doped poly-(methyl methacrylate) films. *Appl. Opt.* **1984**, *23*, 2729–2733. (b) Franke, H.; Heuer, W. Photo-induced self-condensation, a technique for fabricating organic lightguide structures. *Proc. SPIE—Int. Soc. Opt. Eng.* **1986**, *651*, 120–125.

(5) Okamoto, N.; Tashiro, S. Optical waveguides of polymethyl methacrylate doped with benzophenone and coumarin. *Opt. Commun.* **1988**, *66*, 93–96.

(6) (a) Viswanathan, N. K.; Kim, D. Y.; Bian, S.; Williams, J.; Liu, W.; Li, L.; Samuelson, L.; Kumar, J.; Tripathy, S. K. Surface relief structures on azo polymer films. *J. Mater. Chem.* **1999**, *9*, 1941–1955. (b) Oliveira, O. N.; dos Santos, D. S.; Balogh, D. T.; Zucolotto, V.; Mendonca, C. R. Optical storage and surface-relief gratings in azobenzene-containing nanostructured films. *Adv. Colloid Interface Sci.* **2005**, *116*, 179–192.

(7) Gusarov, A. I.; Doyle, D. B. Contribution of photoinduced densification to refractive-index modulation in Bragg gratings written in Ge-doped silica fibers. *Opt. Lett.* **2000**, *25*, 872–874.

(8) Hisakuni, H.; Tanaka, K. Optical microfabrication of chalcogenide glasses. *Science* **1995**, *270*, 974–975.

(9) Sramek, R.; Smektala, F.; Xie, W. X.; Douay, M.; Niay, P. Photoinduced surface expansion of fluorozirconate glasses. *J. Non-Cryst. Solids* **2000**, *277*, 39–44.

(10) Annapoorna, A.; Tokuyuki, H.; Alice, Y. L.; Lambertus, H. Two-photon holographic recording in aluminosilicate glass containing silver particles. *Opt. Lett.* **1997**, *22*, 967–969.

(11) (a) Darracq, B.; Chaput, F.; Lahlil, K.; Lévy, Y.; Boilot, J. P. Photoinscription of surface relief gratings on azo-hybrid gels. *Adv. Mater.* **1998**, *10*, 1133–1136. (b) Landraud, N.; Peretti, J.; Chaput, F.; Lampel, G.; Boilot, J. P.; Lahlil, K.; Safarov, V. I. Near-field optical patterning on azo-hybrid sol–gel films. *Appl. Phys. Lett.* **2001**, *79*, 4562–4564.

(12) Bae, B. S. High photosensitive sol–gel hybrid materials for direct photo-imprinting of micro-optics. *J. Sol-Gel Sci. Technol.* **2004**, *31*, 309–315.

(13) (a) Jang, J. H.; Kang, D. J.; Bae, B. S. Large photoinduced densification in organically modified germanosilicate glasses. *J. Am. Ceram. Soc.* **2004**, *87*, 155–158. (b) Kim, J. K.; Kang, D. J.; Bae, B. S. Wavelength-dependent photosensitivity in a germanium-doped sol–gel hybrid material for direct photopatterning. *Adv. Funct. Mater.* **2005**, *15*, 1870–1876.

(14) (a) Moreau, Y.; Arguel, P.; Coudray, P.; Etienne, P.; Porque, J.; Signoret, P. Direct printing of gratings on sol–gel layers. *Opt. Eng.* **1998**, *37*, 1130–1135. (b) Blanc, D.; Pelissier, S.; Saravanamuttu, K.; Najafi, S. I.; Andrews, M. P. Self-processing of surface relief gratings in photosensitive hybrid sol–gel glasses. *Adv. Mater.* **1999**, *11*, 1508–1511. (c) Blanc, D.; Pélissier, S. Fabrication of sub-micron period diffraction gratings in self-processing sol–gel glasses. *Thin Solid Films* **2001**, *384*, 251–253.

(15) Molina, C.; Moreira, P. J.; Gonçalves, R. R.; Sá Ferreira, R. A.; Messaddeq, Y.; Ribeiro, S. J. L.; Soppera, O.; Leite, A. P.; Marques, P. V. S; de Zea Bermudez, V.; Carlos, L. D. Planar and UV written channel optical waveguides prepared with siloxane-poly(oxyethylene)-zirconia organic/inorganic hybrids. Structure and optical properties. *J. Mater. Chem.* **2005**, *15*, 3937–3945.

(16) (a) Bae, B. S.; Park, O. H.; Charters, R.; Luther-Davies, B.; Atkins, G. R. Direct laser writing of self-developed waveguides in benzyldimethylketal-doped sol–gel hybrid glass. *J. Mater. Res.* **2001**, *16*, 3184–3187. (b) Jung, J. I.; Park, O. H.; Bae, B. S. Fabrication of channel waveguides by photochemical self-developing in doped sol–gel hybrid glass. *J. Sol-Gel Sci. Technol.* **2003**, *26*, 897–901. (c) Park, O. H.; Kim, S. J.; Bae, B. S. Photochemical reactions in fluorinated sol–gel hybrid materials doped with a photolocking agent for direct micropatterning. *J. Mater. Chem.* **2004**, *14*, 1749–1753. (d) Kang, D. J.; Kim, W. S.; Bae, B. S.; Park, H. K.; Jung, B. H. Direct photofabrication of refractive-index-modulated multimode optical waveguide using photosensitive sol–gel hybrid materials. *Appl. Phys. Lett.* **2005**, *87*, 221106.

(17) (a) Park, J. U.; Kim, W. S.; Bae, B. S. Photoinduced low refractive index in a photosensitive organic–inorganic hybrid material. *J. Mater. Chem.* **2003**, *13*, 738–741. (b) Kang, D. J.; Park, J. U.; Bae, B. S.; Nishii, J.; Kintaka, K. Single-step photopatterning of diffraction gratings in highly photosensitive hybrid sol–gel films. *Opt. Expression* **2003**, *11*, 1144–1148.

(18) (a) Kang, D. J.; Kim, J. K.; Bae, B. S. Simple fabrication of diffraction gratings by two-beam interference method in highly photosensitive hybrid sol–gel films. *Opt. Expression* **2004**, *12*, 3947–3953. (b) Kang, D. J.; Phong, P. V.; Bae, B. S. Fabrication of high-efficiency Fresnel-type lenses by pinhole diffraction imaging of sol–gel hybrid materials. *Appl. Phys. Lett.* **2004**, *85*, 4289–4291.

(19) Blanc, D.; Pélissier, S.; Jurine, P. Y.; Soppera, O.; Croutxé-Barghorn, C.; Carré, C. Photo-induced swelling of hybrid sol–gel thin films: Application to surface micro-patterning. *J. Sol-Gel Sci. Technol.* **2003**, *27*, 215–220.

(20) (a) Yu, W.; Yuan, X. C. Volume growth initiated by point-to-point ultraviolet-laser direct writing in hybrid sol–gel glass for three-dimensional microfabrication. *Opt. Lett.* **2003**, *28*, 1573–1575. (b) Yu, W.; Yuan, X. Localized self-volume growth in hybrid sol–gel glass induced by ultraviolet radiation with a gray-scale mask. *Appl. Opt.* **2004**, *43*, 575–578.

(21) (a) Kärkkäinen, A. H. O.; Rantala, J. T.; Maaninen, A.; Jabbour, G. E.; Descour, M. R. Siloxane-based hybrid glass materials for binary and grayscale mask photoimaging. *Adv. Mater.* **2002**, *14*, 535–540. (b) Kärkkäinen, A. H. O.; Tamkin, J. M.; Rogers, J. D.; Neal, D. R.; Hormi, O. E.; Jabbour, G. E.; Rantala, J. T.; Descour, M. R. Direct photolithographic deforming of organomodified siloxane films for micro-optics fabrication. *Appl. Opt.* **2002**, *41*, 3988–3998. (c) Kärkkäinen, A. H. O.; Rantala, J. T.; Tamkin, J. M.; Descour, M. R. Photolithographic processing of hybrid glasses for microoptics. *J. Lightwave Technol.* **2003**, *21*, 614–623.

(22) Kang, D. J.; Jeong, J. P; Bae, B. S. Direct photofabrication of focal-length-controlled microlens array using photoinduced migration mechanisms of photosensitive sol–gel hybrid materials. *Opt. Expression* **2006**, *14*, 8347–8353.

(23) (a) Sinzinger, R.; Jahns, J. *Microoptics*, 2nd ed.; Wiley-VHC: Weinheim, Germany, 2003. (b) Borrelli, N. F. *Microoptics Technology*; Marcel Dekker: New York, 2005.

(24) Sanchez, C.; Ribot, F. Design of hybrid organic–inorganic materials synthesized via sol–gel chemistry. *New J. Chem.* **1994**, *18*, 1007–1047.

(25) Moujoud, A.; Kim, W. S.; Bae, B. S. Thermally stable optical characteristics of sol–gel hybrid materials. *Appl. Phys. Lett.* **2006**, *88*, 101916.

(26) Park, O. H.; Jung, J. I.; Bae, B. S. Photoinduced condensation of sol–gel hybrid glass films doped with benzildimethylketal. *J. Mater. Res.* **2001**, *16*, 2143–2148.

(27) Kim, W. S.; Houbertz, R.; Lee, T. H.; Bae, B. S. Effect of photoinitiator on photopolymerization of inorganic–organic hybrid polymers (ORMOCER). *J. Polym. Sci., Part B: Polym. Phys.* **2004**, *42*, 1979–1986.

AR6000439